Measure of Straight Lines and its Applications in Digital Geometry

David Coeurjolly, Isabelle Sivignon

Measure of Straight Lines and its Applications in Digital Geometry*

David Coeurjolly and Isabelle Sivignon

Université de Lyon, CNRS, LIRIS, UMR5205, F-69622, France
{david.coeurjolly,isabelle.sivignon}@liris.cnrs.fr

Abstract. In digital geometry, objects such as digital straight lines can be considered as equivalent classes of Euclidean straight lines with respect to a digitization process. This paper investigates the analysis of the set of straight lines whose digitization is a given digital straight segment with the help of tools from integral geometry. After a definition of a measure on such sets, we illustrate several applications of it in digital geometry.

1 Introduction

When investigating relationships between Euclidean and Digital geometries, we are facing difficulties induced by the digitization process: Given a digital set $X \subset \mathbb{Z}^2$, there is an infinity of shapes $\Omega_X \subset \mathbb{R}^2$ such that $X = \Omega_X \cap \mathbb{Z}^2$ (in this statement, we have considered the Gauss digitization process [1] for the sake of simplicity). The set Ω_X can be considered as the *preimage* of X for the Gauss digitization. If we want to perform geometrical analysis on digital objects we usually associate properties on X from properties of its preimage set Ω_X. For example, X is digitally convex if there exists a continuous convex shape in Ω_X [2]. In shape analysis, many approaches exist to decide if the set X is digitally straight (see [3] for a survey). Among all the definitions of Digital Straight Lines (DSL for short), we consider the following one: X is a DSL if there exist a Euclidean straight line in Ω_X.

In this paper we focus on the analysis of a subset of Ω_X which only corresponds to straight lines: we define $\mathcal{L}_X$ the set of straight lines (maybe empty) such that the digitization of each line in $\mathcal{L}_X$ is exactly X. Note that we can define a digital straight segment (DSS for short) and its associated preimage as the set of Euclidean lines whose digitization contains X. In the literature, the preimage $\mathcal{L}_X$ has been widely used to control DSS recognition algorithms [4,5,6,3], or to perform geometric reconstruction from a digital contour [7]. In some sense, $\mathcal{L}_X$ can be considered as an uncertainty characterization of X with straight lines: Given a set X, the *thinner* the $\mathcal{L}_X$, the *finer* the DSS characterization of X.

We propose here to formalize and investigate this preimage analysis with the help of integral geometry results [8]. More precisely, we use the mathematical

* This work was partially funded by the ANR project GeoDIB ANR-06-BLAN-0225.

measure of lines in the plane to evaluate a kind of accuracy of the DSS recognition. Similar analyses have been proposed in [9] to compare the continuous and the analytical Hough transforms. The authors have considered the measure of the DSS worst case in both models for recognition purposes. We provide here a closed formula to evaluate the measure of lines and we illustrate several applications in digital geometry.

2 Measure of Straight Lines in the Plane

2.1 Preliminaries

In this section, we first recall integral geometry results [8]. First of all, let us consider a polar representation (ρ, ϕ) of a straight line l with $\phi \in [0, 2\pi]$ and $\rho \geq 0$ Hence, a point $p(x, y) \in \mathbb{R}^2$ belongs to l if

$$x \cos\phi + y \sin\phi - \rho = 0\,.$$

In integral geometry and in the theory of geometrical probability, the measure of a set $\mathcal{L}$ of lines is defined as the integral over the set of a differential form $\omega = f(\rho, \phi) d\rho \wedge d\phi$, provided the fact that this integral exists in the Lebesgue sense. The differential form is defined using notations and rules of the exterior calculus for which an overview is given in [8]. In our context, exterior calculus will coincide with classical differential calculus in most situations.

To define a measure of straight lines, the function f should be chosen such that the resulting integral is invariant under the group of motions in the plane (rotation and translation). In fact, the invariance implies that f is constant [10,8]. Hence using $f(\rho, \phi) = 1$ we have:

Theorem 1 ([8]). *The measure of a set of lines $G(\rho, \phi)$ is defined by the integral over G of the differential form*

$$dG = d\rho \wedge d\phi\,. \tag{1}$$

Note that the measure is always taken at absolute value. In the following, since we will only consider continuous and closed domains G, the integral always exists in the Lebesgue sense. As a consequence, the measure is positive, monotonic (if $A \subseteq B$, then $m(A) \leq m(B)$), additive (if $A \cap B = \emptyset$, then $m(A \cap B) = m(A) + m(B)$), and the measure of the empty set is 0.

2.2 Density in the $(a, b)-$linear space

As defined above, the measure definition perfectly matches with the $(\rho, \phi)-$Hough transform for computer vision purposes [11]. Indeed, given a continuous and closed domain G in the (ρ, ϕ) space, the measure of G is

$$m(G) = \int_G d\rho \wedge d\phi\,, \tag{2}$$

which simply corresponds to the area of G in (ρ, ϕ).

In digital geometry, when considering DSS preimages [4,12,5,6,3], we usually prefer the slope-intercept linear parameter space, denoted $(a, b)-$space in the following, since it allows to characterize arithmetical properties embedded in DSS. This parameter space maps the line $ax - y + b = 0$ to the point (a, b). Conversely, straight lines in the $(a, b)-$space are mapped onto points in the primal space.

In order to obtain the measure of straight lines in this space, we need to perform a transformation in the integral calculus. From [8], we know that if the straight lines are parametrized by their intercept u (resp. v) along the $x-$axis (resp. $y-$axis), we can change the coordinates

$$\begin{cases} \rho = \frac{uv}{\sqrt{u^2+v^2}} \\ \phi = \arctan(u/v) \end{cases} \tag{3}$$

to obtain

$$dG = \frac{uv}{(u^2+v^2)^{\frac{3}{2}}} du \wedge dv\,. \tag{4}$$

If we consider now the (a, b) parametrization widely used in digital geometry, we define the transformation:

$$\begin{cases} u = -\frac{b}{a} \\ v = b \end{cases} \tag{5}$$

and obtain

$$\begin{cases} \rho = \frac{b}{\sqrt{1+a^2}} \\ \phi = \arctan(-\frac{1}{a}) \end{cases} \tag{6}$$

whose Jacobian matrix is

$$J = \begin{bmatrix} \frac{ab}{(1+a^2)^{3/2}} & \frac{1}{\sqrt{1+a^2}} \\ \frac{1}{1+a^2} & 0 \end{bmatrix} \tag{7}$$

Hence,

$$dG = d\rho \wedge d\phi = |det(J)| da \wedge db \tag{8}$$

Finally,

Lemma 1. *The measure of a set of lines $G(a, b)$ is defined by the integral over G of the differential form*

$$dG = \frac{da \wedge db}{(1+a^2)^{\frac{3}{2}}}\,. \tag{9}$$

Even if the $(a, b)-$parametrization leads to a more complex differential form, we demonstrate in the next sections that the measure of DSS preimages in the $(a, b)-$space can be easily computed.

In terms of geometric probability, the measure allows us to obtain interesting properties. For example given two bounded and closed domains Ω and Ω' with $\Omega' \subset \Omega$ and $\Omega, \Omega' \subset \mathbb{R}^2$, the probability that a random line intersects Ω' with the hypothesis that it also intersects Ω is $p = \frac{m(\Omega')}{m(\Omega)}$. For further developments on probability results from a measure, please refer to [8].

2.3 Measure of Lines of a closed (a, b)-space domain

Let us consider a polygonal domain P in the $(a, b)-$space defined by its boundary vertices $\{p_i = (a_i, b_i)\}_{i=0..n-1}$ (counter-clockwise). Given a function f measurable on P (in the Lebesgue sense), a classical way to compute the integral of f over P is to decompose the computation into a finite summation of triangular integration processes. As illustrated in Fig. 1, let T_i be the oriented triangle $\{(0, 0), p_i, p_{(i+1 \ mod \ n)}\}$ for $0 \leq i \leq n - 1$. For each triangle T_i, let δ_i be the sign of its signed area ($\delta_i = \text{sign}(a_i b_{i+1} - a_{i+1} b_i)$).

In the rest of the paper, all index shifts such as $i + j$ must be considered modulo n. Using the above notations

$$\int_P f(a, b) da db = \sum_{i=0}^{n-1} \delta_i \int_{T_i} f(a, b) da db \,. \tag{10}$$

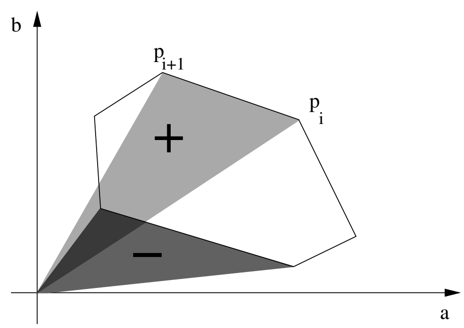

Fig. 1. Integration scheme over a polygonal domain.

The next step is to compute the integration over triangles T_i. To solve that problem, we also consider a linear variable transformation which maps the triangle T_i to the unit triangle $\{(0, 0), (1, 0), (0, 1)\}$

$$\begin{cases} a = a_i a' + a_{i+1} b' \\ b = b_i a' + b_{i+1} b' \end{cases} \text{ whose Jacobian matrix is } J_i = \begin{bmatrix} a_i & a_{i+1} \\ b_i & b_{i+1} \end{bmatrix} \tag{11}$$

Thus

$$\int_{T_i} f(a, b) da db = |det(J_i)| \int_0^1 \int_0^{1-b'} f(a', b') da' db' \tag{12}$$

Note that the sign of $det(J_i)$ and δ_i coincides. Finally, we obtain the following lemma:

Lemma 2. *The measure of a set of straight lines defined in a polygonal domain $P = \{a_i, b_i)\}_{i=0..n-1}$ in the (a, b)-space is*

$$m(P) = \sum_{i=0}^{n-1} (a_i b_{i+1} - a_{i+1} b_i) \cdot g(a_i, a_{i+1}) \tag{13}$$

with

$$g(a_i, a_{i+1}) = \begin{cases} \frac{1}{1+a_i^2+\sqrt{1+a_i^2}} & \textit{if } a_i = a_{i+1}, \\ \frac{1}{1+\sqrt{1+a_i^2}} & \textit{if } a_{i+1} = 0, \\ \frac{1}{1+\sqrt{1+a_{i+1}^2}} & \textit{if } a_i = 0, \\ \frac{a_{i+1}-\sqrt{1+a_i^2}a_{i+1}+a_i\left(-1+\sqrt{1+a_{i+1}^2}\right)}{a_i a_{i+1}(a_{i+1}-a_i)} & \textit{otherwise.} \end{cases} \tag{14}$$

Proof. With Eq. (9), (10) and (12), we have

$$m(P) = \sum_{i=0}^{n-1}(a_i b_{i+1} - a_{i+1} b_i) \int_0^1 \int_0^{1-b'} \frac{da' db'}{(1 + (a_i.a' + a_{i+1}.b')^2)^{\frac{3}{2}}} \tag{15}$$

Then, thanks to the mapping of T_i triangles to the unit triangle, the rightmost integral term can be evaluated to obtain closed formulas presented in Eq. (14). The function $g(a_i, a_{i+1})$ in the lemma statement defines the result of the integral computation obtained by a symbolic mathematical solver. □

3 Measure of Digital Straight Segments and Applications

3.1 DSS Preimage and Farey Fan

In the following, we use the preimage definition proposed by Lindenbaum and Bruckstein [6]. Consider a straight line $y = a_0 x + b_0$ (without loss of generality, $(a_0, b_0) \in [0, 1] \times [0, 1[$, *i.e.* straight lines are supposed to be in the first octant), the digitization of this line using the Object Boundary Quantization (see [13] for a survey on digitization schemes) on an unit grid is the set of discrete points such that $X = \left\{(x, y) \in \mathbb{Z}^2 \mid \lfloor a_0 x + b_0 - y \rfloor = 0\right\}$. The preimage of X is thus defined by

$$\mathcal{L}_X = \{(a, b) \in [0, 1] \times [0, 1[\mid \forall (x, y) \in X,\ y \leq ax + b < y + 1\}. \tag{16}$$

In the (a, b)-space $\mathcal{L}_X$ is a convex polygon whose vertices are embedded in a strong arithmetical structure, the Farey Fan [12]. Indeed, each pixel in X induces two linear constraints with integer coefficients. The Farey Fan of order n is the arrangement obtained as the intersection of all possible linear constraints associated to pixels in $[0, n] \times [0, n]$. In other words, it is the arrangement of the set of lines $\{y/x,\ 0 \leq y \leq x, 1 \leq x \leq n\}$ in the domain $[0, 1] \times [0, 1]$ [12]. The vertex coordinates of this arrangement are irreducible fractions whose denominator is less or equal to n. Finally, such an arithmetical structure allows us to design fast recognition algorithms since the cells in the Farey Fan of order n defines all DSS of length $n + 1$ in the first octant[5,6].

A first application of the measure is to merge both arithmetical properties and *uncertainty* within the same framework. Indeed, each cell of a Farey Fan of order n represents a DSS X of length $n + 1$. With the measure associated to this preimage (and thus to X), we can evaluate the quantity (in terms of integral measure) of straight lines whose digitization contains X. Hence, Fig. 3 illustrates Farey Fans of order from 0 to 5 in which the gray value corresponds to the measure computed with Lemma 2 on each cell (the white color cell is the preimage with maximal measure). As expected, we can observe that the cells have a high variability with respect to the measure. If we consider DSS examples in Fig. 2, both DSS preimages are in the Farey Fan of order 4 (Fig. 3-(e)). However, if we consider the following probability test: given a random straight line l whose slope and intercept is in $[0, 1] \times [0, 1]$, the probability such that the digitization of l contains the left DSS is 3.7 times higher than the probability of the right DSS. Hence, the measure is a powerful tool to perform *a posteriori* evaluation of DSS recognitions.

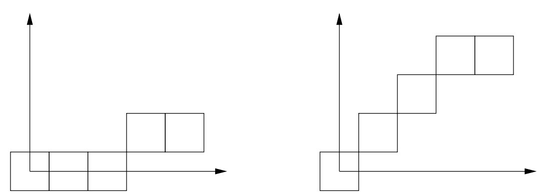

Fig. 2. Two DSS of length 5 with measure respectively 0.0738 (left) and 0.0198 (right).

3.2 Representative Euclidean Straight Line of a DSS

In applications such as the polygonal reconstruction from a digital curve, we sometimes need to associate a representative Euclidean straight line to a preimage. In the literature, such a representative straight line is usually computed as the point in the $(a, b)-$space defined as the mid-point of the preimage diagonal obtained by the two vertices of equal abscissa [14]. The advantage of such an approach is that both the obtained straight line and the DSS slopes are identical.

We propose here a new definition of the representative Euclidean straight line based on integral geometry tools.

Definition 1. *Given a continuous and closed domain $G(a, b)$, the representative Euclidean Straight Line is the center of mass of G on the density function defined in Sect. 2.2. In other words, such a point is defined as*

$$\left(\frac{\int_G \ a \ dadb}{\int_G dadb}, \frac{\int_G \ b \ dadb}{\int_G dadb} \right) \tag{17}$$

In terms of probability, the centroid definition corresponds to the expected values of the normalized probability distributions defined from the density on the a and b variables in the Lebesgue sense.

The denominators in Eq. (17) correspond to the measure G. To evaluate the numerators on a polygonal domain P, we can use the evaluation scheme detailed in Sect. 2.3: we decompose the integration over P into a finite sum of integrations over the unit triangle. Finally, we evaluate the integrals to obtain closed formulas.

Lemma 3. *The Representative Euclidean straight line of a polygonal domain* $P = \{(a_i, b_i)\}_{i=0..n-1}$ *in the* $(a, b)-$*space is the point* $(\frac{C_a}{m(P)}, \frac{C_b}{m(P)})$ *with*

$$C_a = \sum_{i=0}^{n-1} (a_i b_{i+1} - a_{i+1} b_i) \cdot g_a(a_i, a_{i+1})$$

$$C_b = \sum_{i=0}^{n-1} (a_i b_{i+1} - a_{i+1} b_i) \cdot g_b(a_i, a_{i+1}, b_i, b_{i+1})$$

and

$$g_a(a_i, a_{i+1}) = \begin{cases} \frac{arcsinh(a_i) - \frac{a_i}{\sqrt{1+a_i^2}}}{a_i^2} & \text{if } a_i = a_{i+1}, \\ \frac{a_{i+1} - arcsinh(a_{i+1})}{a_{i+1}^2} & \text{if } a_i = 0, \\ \frac{a_i - arcsinh(a_i)}{a_i^2} & \text{if } a_{i+1} = 0, \\ \frac{a_i\, arcsinh(a_{i+1}) - a_{i+1}\, arcsinh(a_i)}{a_i a_{i+1} (a_i - a_{i+1})} & \text{otherwise.} \end{cases}$$

$$g_b(a_i, a_{i+1}, b_i, b_{i+1}) = \begin{cases} \frac{(b_i + b_{i+1})\, arcsinh(a_i) - \frac{a_i \left(b_i + a_i \left(-a_i + \sqrt{1+\frac{1}{a_i^2}}\sqrt{1+a_i^2}\right) b_{i+1}\right)}{\sqrt{1+a_i^2}}}{2a_i^3} & \text{if } a_i = a_{i+1}, \\ \frac{a_{i+1}\left(\left(-2+\sqrt{1+a_{i+1}^2}\right) b_i + 2b_{i+1}\right) + (b_i - 2b_{i+1})\, arcsinh(a_{i+1})}{2a_{i+1}^3} & \text{if } a_i = 0, \\ \frac{a_i \left(2b_i + \left(-2+\sqrt{1+a_i^2}\right) b_{i+1}\right) + (-2b_i + b_{i+1})\, arcsinh(a_i)}{2a_i^3} & \text{if } a_{i+1} = 0, \\ NumApprox(a_i, a_{i+1}, b_i, b_{i+1}) & \text{otherwise.} \end{cases}$$

where $NumApprox(a_i, a_{i+1}, b_i, b_{i+1})$ *is the numerical approximation of*

$$\int_0^1 \int_0^{1-b'} \frac{(b_i a' + b_{i+1} b') da' db'}{(1 + (a_i.a' + a_{i+1}.b')^2)^{\frac{3}{2}}} \tag{18}$$

The proof of this lemma is similar to the proof of Lemma 2: g_a and g_b functions are obtained using a formal integration over the unit triangle. A specific point concerns the g_b function in the general case for which no closed formula has yet been found: we failed to find a suitable parameter transformation in order to help the symbolic integrator to find a solution. However, a closed formula exists to integrate the function in Eq. (18) over a rectangular domain. Hence, the integral can be approximated using the Rectangle Approximation method (function $NumApprox$). Figure 3 illustrates the center of mass for each preimage in Farey Fans of order from 0 to 5. In Fig. 4, we compare our rep-

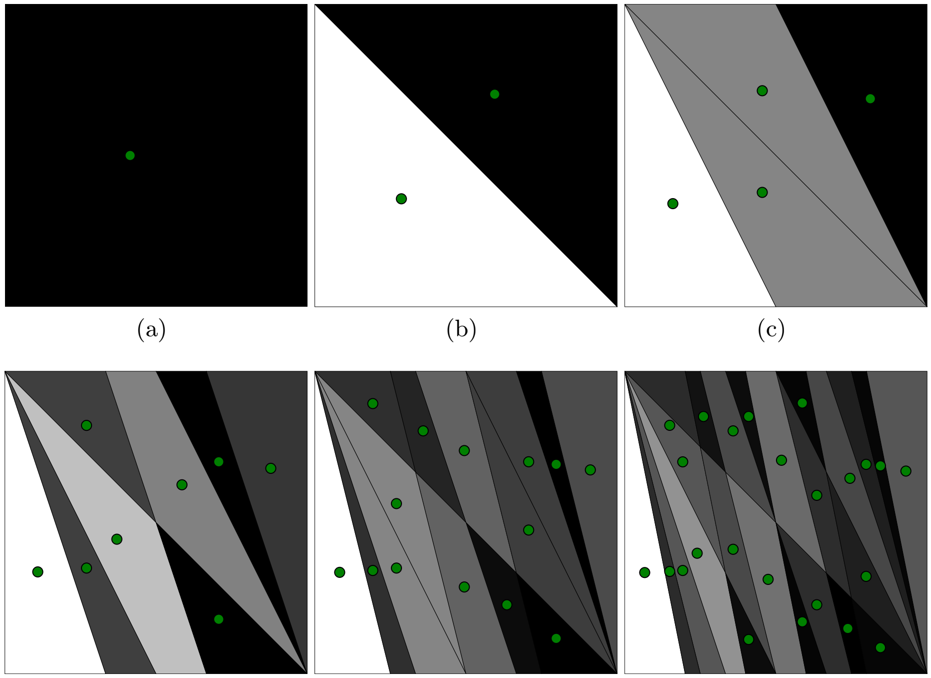

(a) (b) (c)

(d) (e) (f)

Fig. 3. Farey Fan of order from 0 to 5 ($(a) - (f)$) with the center of mass for each preimage. The color corresponds to a linear mapping between the preimage measure and the gray level map (the white color cell is the preimage with maximal measure).

resentative line computation to the one proposed in [14] on the Farey Fan of order 4 (Fig. 4-(a)). Note that even if points in the $(a, b)-$space associated to the representative lines in both definitions may differ, the associated lines in the primal space may be *visually* close. Furthermore, thanks to the definition of the preimage in Eq. (16), both the restriction to positive slope straight lines ($a \in [0, 1]$) and the OBQ digitization scheme make the representative line for horizontal digital segment shifted and not perfectly horizontal (see Fig. 4-(b)). Despite, the proposed representative line definition is consistent to the straight line measure theory. Furthermore, the proposed framework can be generalized to different DSS preimage defintions, including for example, lines with negative slopes or the Gauss digitization model (see Sec. 1)

3.3 Contour analysis with Digital Tangent and Preimage Measures

In this section, we provide a last illustration of the power of the measure to analyze contours. Let us denote by $C = \{p_0, \ldots, p_{n-1}\}$ a digital closed curve.

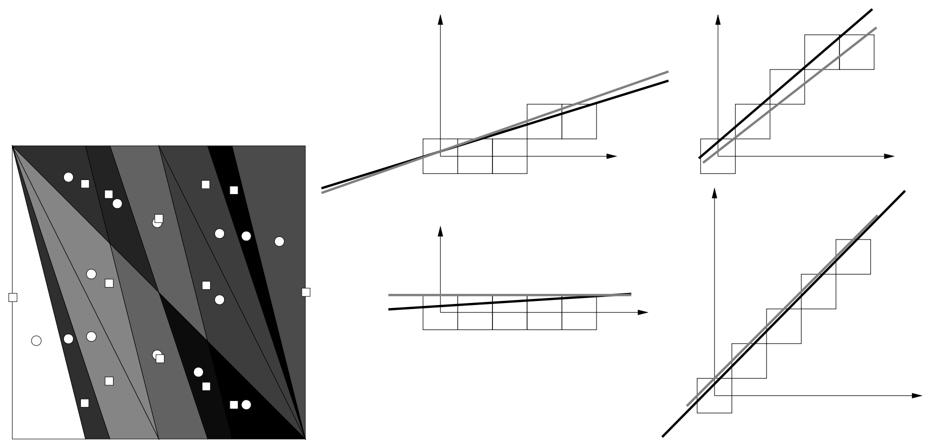

Fig. 4. Comparison between the proposed representative straight line computation (circles in (a) and bold lines (b)) and the existing approach (squares in (a) and gray lines in (b)): (a) differences depicted in the Farey Fan of order 4 and (b) in the primal space.

We consider $N_k(i)$ the sequence $\{p_{i-k}, \ldots, p_i, \ldots, p_{i+k}\}$ (again, index shifts are computed modulo n). From the measure definition detailed above, we can design the following *linearity map*.

Definition 2 (Linearity map). *Given a closed contour C, the linearity map is a function $\lambda : C \to \mathbb{R}$ that associates for each point $p_i \in C$, the measure of straight lines of $N_k(i)$.*

From this definition, several observations can be made:

- if $\lambda(i) = 0$, it means that $N_k(i)$ is not a DSS since there is no Euclidean straight line whose digitization contains $N_k(i)$;
- if $\lambda(i) > \lambda(j)$, it means that the set of straight lines whose digitization contains $N_k(i)$ is *wider* than the set of straight lines whose digitization contains $N_k(j)$.

Roughly speaking, the linearity map measures the *uncertainty* of $N_k(i)$ with respect to the straight lines. From a computational point of view, to compute the λ function, we just have to compute the measures in the Farey Fan of order $2k$ which gives us the set of patterns of length $2k+1$ whose measure is not null (up to symmetry and translation). Then, we scan the sequences of $2k+1$ pixels in C and associate the corresponding measure.

Figures 5 (b) and (d) illustrate the linearity map computed from local patterns of length $2k+1 = 5$ from the kangaroo curve (Figure 5(a)). In Fig. 5(b) and (c) the grey map represents the measure computed for each pixel: white stands for high values while black pixels have a low measure. Cross marked pixels are those for which the local pattern of length 5 is not a digital segment. Local artefacts due to the fixed length of the local patterns can be observed on the "steps" of the curve (vertical or horizontal pixel sequences). In Fig. 5(d), the $\lambda(i)$ graph computed for the kangaroo curve is depicted. Note that high values generally correspond to central pixels of the steps. Indeed, such steps are associated to the highest measure value in the Farey Fan of order 4. To perform a finer analysis of digital contours, it would be of interest to locally adapt the size of the patterns.

In the literature, to design curvature or tangent estimators [15,16] or to extract a minimal DSS decomposition of a digital contours [17], the concept of discrete tangential cover has been widely used to avoid the k parameter. More precisely, given a closed digital contour C, a discrete tangent at a point $p \in C$ is the longest DSS centered at p (see [14] for a more formal definition). In that case, we can also define a linearity map computed on the discrete tangent (in some sense, the neighborhood $N_k(i)$ is adapted locally). Figures 5(c) and (e) illustrate preliminary results obtained using the discrete tangents to compute the measure at each pixel. Note that compared to Fig. 5(b) and (d), the behavior of the measure along the curve is smoother, and that each pixel is now assigned a measure value. The $\lambda(i)$ graph using discrete tangents is depicted in Fig. 5(e). Contrary to the $\lambda(i)$ graph computed from local patterns (Fig. 5(b)), the high values of the measure now seem to match some high curvature parts of the curve. As mentioned above, the linearity map seems to be a complementary tool to the curvature estimation.

4 Conclusion and Future Works

In this paper, we have introduced concepts from integral geometry and geometric probability in the digital geometry context. More precisely, we have focused on the computation of the measure of straight lines in the (a, b) parameter space which allows to first have a precise analysis of Farey Fans in terms of measure. Then, we have investigated a formal and consistent definition of a representative Euclidean straight line associated to a DSS. Finally, we have defined a new tool, so called the linearity map, to describe discrete contours. At this point, only a preliminary analysis of this feature map has been addressed. A formal comparison between such a tool and a classical curvature based descriptor is a challenging future work. Furthermore, it would be interesting to consider similar integral geometry analysis of other objects such as digital circles or digital polynomials.

References

1. Klette, R., Rosenfeld, A.: Digital Geometry: Geometric Methods for Digital Picture Analysis. Series in Computer Graphics and Geometric Modelin. Morgan Kaufmann (2004)

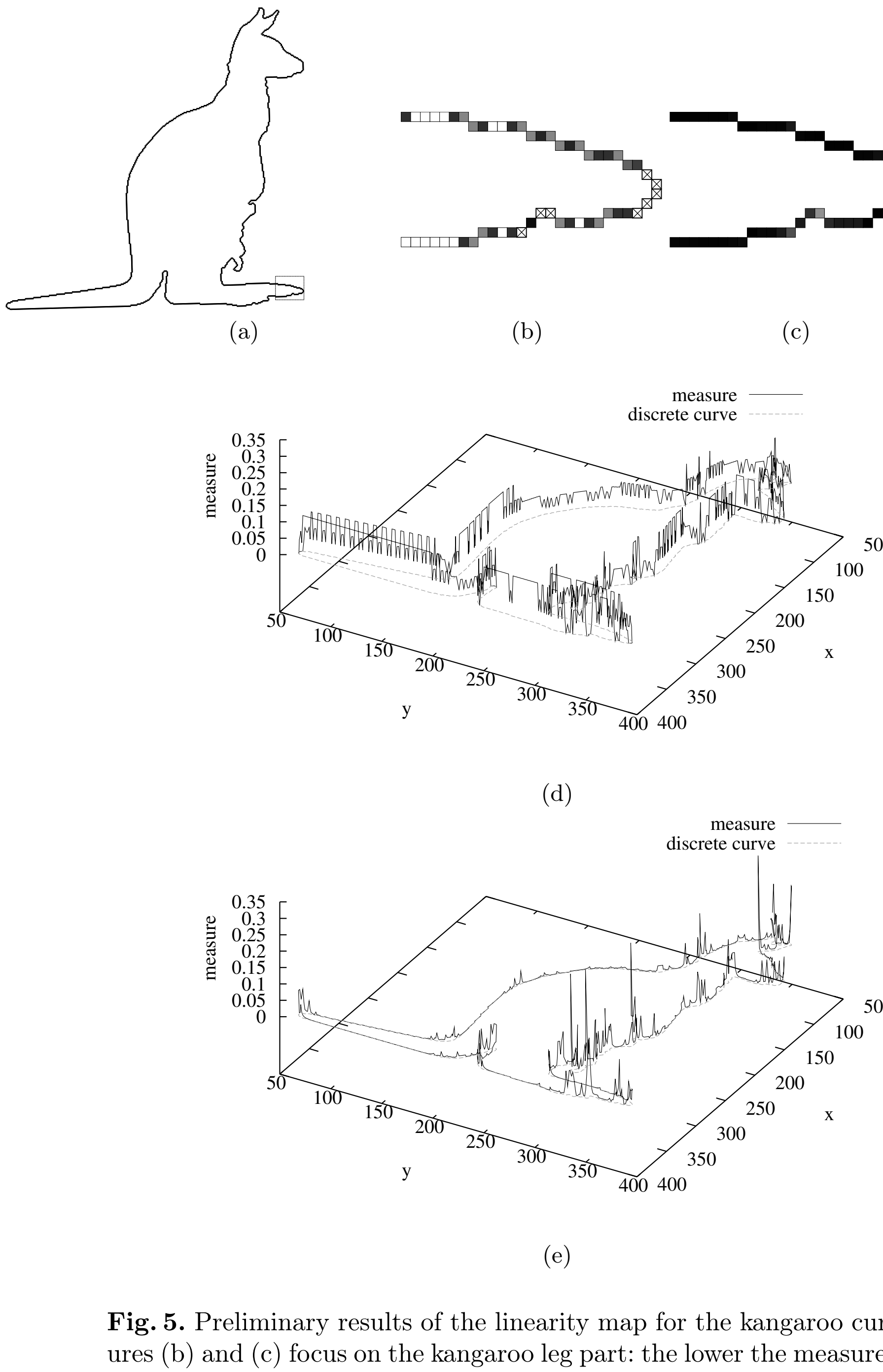

Fig. 5. Preliminary results of the linearity map for the kangaroo curve (a). Figures (b) and (c) focus on the kangaroo leg part: the lower the measure, the darker the pixel. In (b) and (d), local patterns are used to compute the measure, while discrete tangents are used in (c) and (e).

2. Sklansky, J.: Measuring concavity on a rectangular mosaic. IEEE Trans. Computer **21**(12) (dec 1972) 1355–1364
3. Klette, R., Rosenfeld, A.: Digital straightness–a review. Discrete Applied Mathematics **139**(1-3) (APR 2004) 197–230
4. Dorst, L., Smeulders, A.N.M.: Discrete representation of straight lines. IEEE Trans. on Pattern Analysis and Machine Intelligence **6** (1984) 450–463
5. Dorst, L., Smeulders, A.W.M.: Decomposition of discrete curves into piecewise straight segments in linear time. In: Contemporary Mathematics. Volume 119. (1991)
6. Lindenbaum, M., Bruckstein, A.: On recursive, $o(n)$ partitioning of a digitized curve into digital straigth segments. IEEE Trans. on Pattern Analysis and Machine Intelligence **15**(9) (sep 1993) 949–953
7. Breton, R., Sivignon, I., Dupont, F., Andres, E.: Towards an invertible euclidean reconstruction of a discrete object. In Nyström, I., Baja, G.S.d., Svensson, S., eds.: DGCI. Volume 2886 of Lecture Notes in Computer Science., Springer (2003) 246–256
8. Santaló, L.A.: Integral Geometry and Geometric Probability. Volume 1 of Encyclopedia of Mathematics and Its Applications. Addison-Wesley (1985)
9. Kiryati, N., Lindenbaum, M., Bruckstein, A.M.: Digital or analog hough transform? Pattern Recognition Letters **12**(5) (1991) 291–297
10. Crofton, M.: On the theory of local probability. Phil. Trans. of the Royal Soc. (1868) 181–199
11. Duda, R.O., Hart, P.E.: Use of the hough transform to detect lines and curves in pictures. Communications of the ACM **15**(1) (1972) 11–15
12. McIlroy, M.D.: A note on discrete representation of lines. AT&T Technical Journal **64**(2) (FEB 1985) 481–490
13. Jonas, A., Kiryati, N.: Digital representation schemes for 3d curves. Pattern Recognition **30**(11) (1997) 1803–1816
14. Vialard, A.: Geometrical parameters extraction from discrete paths. In: 6th Discrete Geometry for Computer Imagery, Springer-Verlag, LNCS, 1176 (1996) 24–35
15. Lachaud, J.O., Vialard, A., Vieilleville, F.c.d.: Analysis and comparative evaluation of discrete tangent estimators. In Andres, E., Damiand, G., Lienhardt, P., eds.: DGCI. Volume 3429 of Lecture Notes in Computer Science., Springer (2005) 240–251
16. Lachaud, J.O., Vialard, A., Vieilleville, F.d.: Fast, accurate and convergent tangent estimation on digital contours. Image and Vision Computing **25**(10) (oct 2007) 1572–1587
17. Feschet, F., Tougne, L.: On the min dss problem of closed discrete curves. Discrete Applied Mathematics **151**(1-3) (2005) 138 – 153 IWCIA 2003-Ninth International Workshop on Combinatorial Image Analysis.